European Journal of Nuclear Medicine and Molecular Imaging (2019) 46:831–837
https://doi.org/10.1007/s00259-019-4259-5

ORIGINAL ARTICLE

Prediction of biological characteristics of breast cancer using dual-phase FDG PET/CT

Shinsuke Sasada[1] · Norio Masumoto[1] · Eri Suzuki[1] · Satoshi Sueoka[1] · Noriko Goda[1] · Keiko Kajitani[1] · Akiko Emi[1] · Takayuki Kadoya[1] · Morihito Okada[1]

Received: 24 August 2018 / Accepted: 2 January 2019 / Published online: 16 January 2019

Abstract

Purpose The aim of this study was to assess whether the retention index (RI) determined using dual-phase ^{18}F-fluorodeoxyglucose positron emission tomography/computed tomography (FDG PET/CT) reflects the malignant features of breast cancer.

Methods A total of 1,523 patients with breast cancer were retrospectively evaluated. PET/CT scans were performed at 1 h and 2 h after FDG administration before treatment. The maximum standardized uptake value (SUVmax) at both time points (SUVmax1 and SUVmax2) in the primary tumour and RI were calculated. Primary tumour tissues were evaluated in terms of biological features, such as histology, nuclear grade, lymphovascular invasion and molecular subtype.

Results Of the 1,523 patients, 463 (30.4%) had luminal A-like, 661 (43.4%) had luminal B-like, 229 (15.0%) had human epidermal growth factor receptor 2-positive (HER2-positive), and 157 (10.3%) triple-negative breast cancer. The median SUVmax1, SUVmax2 and RI values were 2.2, 2.3 and 2.6%, respectively. These metabolic parameters were correlated with tumour size, nodal metastasis, histology, nuclear grade, lymphovascular invasion, and molecular subtype (all $P < 0.001$). The median RI values were 0% in luminal A-like, 5.3% in luminal B-like, 6.9% in HER2-positive, and 11.4% in triple-negative breast cancer. RI was associated with malignant features when the tumour accumulated a significant amount of FDG. In a subanalysis of patients with tumours of stages T2 to T4, RI was correlated with nodal metastasis, histology, nuclear grade, and molecular subtype (luminal A-like 4.8%, luminal B-like 12.3%, HER2-positive 15.8%, and triple-negative 16.3%).

Conclusion RI determined using delayed-phase FDG PET/CT is associated with malignant features in breast cancers with significant FDG uptake. Dual-phase imaging was helpful in distinguishing luminal A-like breast cancer from luminal B-like, HER2-positive, and triple-negative breast cancers.

Keywords Breast cancer · PET · FDG · Dual-phase · Retention index

Introduction

Breast cancer is the most common cancer affecting adult women worldwide and accounts for approximately 30% of the total cancer incidence [1]. Breast cancer is a heterogeneous disease, and the treatment is decided based on the biological features, such as hormone receptor status, human epidermal growth factor receptor 2 (HER2) status, Ki-67 labelling index, and grade [2]. These biological parameters are recognized as risk factors for recurrence after surgery [3].

^{18}F-FDG PET/CT is a molecular imaging technique based on glucose metabolism. FDG PET/CT is a more useful modality for detecting distant metastases in patients with breast cancer than conventional imaging [4, 5]. Accumulation of FDG increases over time, up to 4–5 h after administration in malignant tumours, and high-contrast images are acquired in the delayed phase [6–8]. In contrast, the uptake of ^{18}F-FDG in inflammatory lesions and normal breast tissues decreases over time [9]. Some studies have shown that the retention index (RI) determined using dual-phase FDG PET/CT is more related to the molecular subtype, biological parameters, and diagnostic accuracy than the single-point standardized uptake value (SUV) in breast cancer [10–12]. However, others have

✉ Shinsuke Sasada
shsasada@hiroshima-u.ac.jp

[1] Department of Surgical Oncology, Research Institute for Radiation Biology and Medicine, Hiroshima University, 1-2-3 Kasumi, Minami-Ku, Hiroshima City, Hiroshima 734-8551, Japan

indicated that RI does not predict the pathological prognostic factors and molecular subtype [13, 14]. The significance of RI in the identification of biological parameters of breast cancer is unclear.

We evaluated whether RI determined using dual-phase FDG PET/CT reflects the biological parameters in a large cohort of patients with breast cancer.

Materials and methods

Patients

Consecutive patients with operable breast cancer who underwent dual-phase FDG PET/CT before treatment between April 2006 and June 2018 were included in the present study. Patients who received neoadjuvant chemotherapy were eligible. Tumour staging was based on the seventh edition of the American Joint Committee on Cancer (AJCC) [15].

The Institutional Review Board of Hiroshima University Hospital (Hiroshima, Japan) approved this study. All procedures performed in human participants were in accordance with the ethical standards of the Institutional Research Committee and with the principles of the 1964 Declaration of Helsinki and its later amendments or comparable ethical standards. Given the retrospective nature of the present study and the use of anonymized patient data, the requirement for informed consent was waived.

FDG PET/CT examination

Patients fasted for at least 4 h before undergoing PET. PET examinations were performed using an integrated Discovery ST16 PET/CT scanner (GE Healthcare, Little Chalfont, UK; bismuth germanate/6.25 × 6.25 × 30 mm). All patients underwent dual time-point scans. The first acquisition was a whole-body scan from the head to the thighs performed 1 h after intravenous administration of 3–3.7 MBq/kg FDG. The second acquisition, which was performed 2 h after FDG injection, imaged only the thoracic region [16]. Low-dose nonenhanced CT images (3–4 mm slices) were acquired for attenuation correction and localization of lesions identified on PET. Immediately after the CT examination, the identical axial field of view (154 mm) was scanned using PET for 2–3 min per table position depending on the patient condition and scanner performance. The acquired data were reconstructed as 128 × 128 matrix images (pixel size, 4.7 × 3.25 mm) using Fourier rebinning and ordered-subsets expectation maximization algorithms. Both PET and CT studies were performed with the patient performing normal tidal breathing and in the supine position.

The PET images were evaluated and the maximum single-voxel SUV quantified using a Xeleris workstation, version 1.1452 (GE Healthcare, USA). Regions of interest were delineated within the primary breast tumour on attenuation-corrected FDG PET images, and the SUVmax was measured. SUVmax semiquantitative parameters from the first and second scans were defined as SUVmax1 and SUVmax2, respectively. RI was calculated using the following expression:

$$(\mathrm{SUVmax2}-\mathrm{SUVmax1}/\mathrm{SUVmax1}) \times 100$$

RI was classified into negative (including no change) and positive subgroups. All PET images were reviewed by two specialists, a nuclear medicine specialist and a breast cancer specialist.

Table 1 Patient characteristics

Characteristic	Value
Age (years), median (range)	59 (23–92)
T status, *n* (%)	
Tis	199 (13.1)
T1	824 (54.1)
T2	419 (27.5)
T3	45 (2.9)
T4	36 (2.4)
N status, *n* (%)	
N0	1100 (72.2)
N1	315 (20.7)
N2	67 (4.4)
N3	41 (2.7)
Histology, *n* (%)	
Noninvasive carcinoma	199 (13.1)
Microinvasive carcinoma	52 (3.4)
Invasive carcinoma of no special type	1122 (73.6)
Invasive lobular carcinoma	30 (2.0)
Other	120 (7.9)
Nuclear grade, *n* (%)	
1	271 (17.8)
2	624 (41.0)
3	626 (41.1)
Unknown	2 (0.1)
Lymphovascular invasion, *n* (%)	
Negative	977 (64.1)
Positive	358 (23.5)
Unknown	188 (12.4)
Subtype, *n* (%)	
Luminal A-like	463 (30.4)
Luminal B-like	661 (43.4)
HER2-positive	229 (15.0)
Triple-negative	157 (10.3)

HER2 human epidermal growth factor receptor 2

Table 2 Relationship between metabolic and biological parameters

Parameter	SUVmax1		SUVmax2		RI (%)	
	Median (IQR)	*P* value	Median (IQR)	*P* value	Median (IQR)	*P* value
T status		<0.001		<0.001		<0.001
Tis	1.5 (1.1–2.0)		1.3 (1.0–1.8)		−7.1 (−18.8 to 0.0)	
T1	1.9 (1.3–3.0)		1.8 (1.2–3.1)		0.0 (−11.1 to 11.8)	
T2	4.2 (2.7–6.6)		4.7 (2.8–7.9)		12.2 (1.9–20.6)	
T3	4.6 (3.0–7.6)		5.3 (3.1–9.0)		13.9 (2.6–18.9)	
T4	5.6 (4.2–8.9)		6.7 (4.8–11.0)		15.6 (9.6–21.8)	
N status		<0.001		<0.001		<0.001
N0	1.9 (1.3–3.1)		1.8 (1.2–3.3)		0.0 (−11.8 to 12.0)	
N1	3.5 (2.1–5.5)		3.9 (2.1–6.5)		10.5 (0.0–19.0)	
N2	4.2 (2.5–5.9)		4.5 (2.5–7.2)		11.8 (0.0–18.1)	
N3	6.2 (3.5–8.6)		6.6 (4.1–10.1)		16.2 (6.5–26.9)	
Histology		<0.001		<0.001		<0.001
Noninvasive carcinoma	1.5 (1.1–2.0)		1.3 (1.0–1.8)		−7.1 (−18.8 to 0.0)	
Microinvasive carcinoma	1.7 (1.2–2.2)		1.5 (1.1–2.1)		−5.9 (−16.3 to 0.0)	
Invasive carcinoma of no special type	2.7 (1.6–4.8)		2.8 (1.6–5.5)		6.8 (−5.5 to 16.7)	
Invasive lobular carcinoma	1.8 (1.1–2.7)		1.7 (1.1–2.6)		−3.8 (−13.7 to 3.6)	
Other	1.9 (1.3–3.0)		1.8 (1.1–3.1)		0.0 (−15.5 to 11.3)	
Nuclear grade		<0.001		<0.001		<0.001
1	1.5 (1.1–2.0)		1.3 (0.9–2.0)		−7.1 (−16.7 to 5.6)	
2	2.0 (1.4–3.3)		1.3 (1.4–3.7)		0.0 (−10.6 to 14.2)	
3	3.2 (1.9–5.7)		3.6 (1.9–6.5)		8.3 (0.0–17.8)	
Lymphovascular invasion		<0.001		<0.001		<0.001
Negative	1.9 (1.3–3.0)		1.7 (1.1–3.3)		0.0 (−14.3 to 12.1)	
Positive	2.9 (1.9–4.4)		3.1 (1.9–5.0)		7.8 (0.0–17.4)	
Molecular subtype		<0.001		<0.001		<0.001
Luminal A-like	1.6 (1.2–2.4)		1.5 (1.0–2.5)		0.0 (−14.0 to 7.7)	
Luminal B-like	2.5 (1.6–4.3)		2.6 (1.5–4.8)		5.3 (−7.1 to 15.2)	
HER2-positive	3.1 (1.9–5.5)		3.4 (1.7–6.3)		6.9 (−4.1 to 17.5)	
Triple-negative	4.0 (1.7–7.5)		4.7 (1.5–9.0)		11.4 (−3.7 to 21.4)	

HER2 human epidermal growth factor receptor 2, *IQR* interquartile range, *RI* retention index, *SUVmax* maximum standardized uptake value

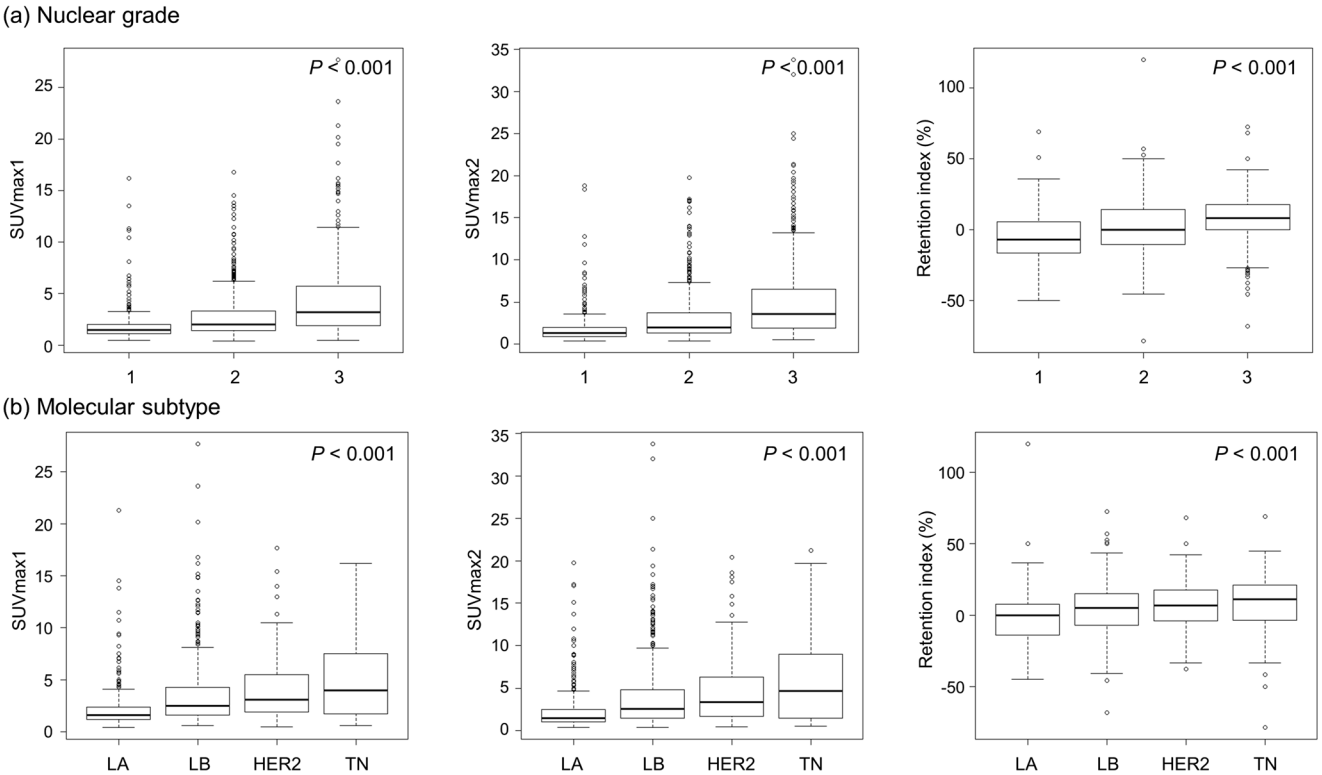

Fig. 1 Relationships between metabolic parameters and nuclear grade (**a**) and molecular subtype (**b**). *HER2* human epidermal growth factor receptor 2, *LA* luminal A-like, *LB* luminal B-like, *TN* triple-negative

Table 3 Relationship between RI and biological parameters in relation to background SUVmax

	Total			SUVmax1 <1.4			SUVmax1 ≥1.4		
	Negative RI ($n = 747$)	Positive RI ($n = 776$)	*P* value	Negative RI ($n = 288$)	Positive RI ($n = 56$)	*P* value	Negative RI ($n = 459$)	Positive RI ($n = 720$)	*P* value
T status			<0.001			0.615			<0.001
Tis	159 (21.3)	40 (5.2)		74 (25.8)	13 (23.2)		85 (18.5)	27 (3.8)	
T1	470 (62.9)	354 (45.6)		195 (67.7)	39 (69.6)		275 (59.9)	315 (43.7)	
T2	102 (13.7)	317 (40.9)		17 (5.9)	3 (5.4)		85 (18.5)	314 (43.6)	
T3	11 (1.5)	34 (4.4)		1 (0.3)	0 (0)		10 (2.2)	34 (4.7)	
T4	5 (0.7)	31 (4.0)		1 (0.3)	1 (1.8)		4 (0.9)	30 (4.2)	
N status			<0.001			0.017			<0.001
N0	630 (84.3)	470 (60.6)		273 (94.8)	47 (83.9)		357 (77.8)	423 (58.8)	
N1	91 (12.2)	224 (28.9)		12 (4.2)	8 (14.3)		79 (17.2)	216 (30.0)	
N2	18 (2.4)	49 (6.3)		2 (0.7)	1 (1.8)		16 (3.5)	48 (6.7)	
N3	8 (1.1)	33 (4.3)		1 (0.3)	0 (0)		7 (1.5)	33 (4.6)	
Nuclear grade			<0.001			0.769			<0.001
1	195 (26.1)	76 (9.8)		100 (34.7)	18 (32.7)		95 (20.7)	58 (8.1)	
2	335 (44.8)	289 (37.3)		127 (44.1)	23 (41.8)		208 (45.3)	266 (37.0)	
3	217 (29.0)	409 (52.8)		61 (21.2)	14 (25.5)		156 (34.0)	395 (54.9)	
Lymphovascular invasion			<0.001			0.017			<0.001
Negative	589 (83.3)	388 (61.8)		264 (92.6)	44 (81.5)		325 (77.0)	344 (59.9)	
Positive	118 (16.7)	240 (38.2)		21 (7.4)	10 (18.5)		97 (23.0)	230 (40.1)	
Subtype			<0.001			0.813			<0.001
Luminal A-like	308 (41.7)	155 (20.1)		144 (50.5)	28 (50.0)		164 (36.2)	127 (17.7)	
Luminal B-like	285 (38.6)	376 (48.7)		90 (31.6)	19 (33.9)		195 (43.0)	357 (49.9)	
HER2-positive	88 (11.9)	141 (18.3)		25 (8.8)	6 (10.7)		63 (13.9)	135 (18.9)	
Triple-negative	57 (7.7)	100 (13.0)		26 (9.1)	3 (5.4)		31 (6.8)	97 (13.5)	

HER2 human epidermal growth factor receptor 2, *RI* retention index, *SUVmax* maximum standardized uptake value

Pathological assessment

Breast tumour samples were collected via core-needle biopsy or surgery. Histological assessment was performed using the surgical specimens. In patients who underwent neoadjuvant chemotherapy, the biopsy specimens before treatment were evaluated. The histology, nuclear grade, lymphovascular invasion (LVI) and nodal metastasis were determined using tumour slices stained with haematoxylin and eosin. Oestrogen receptor (ER) and HER2 levels were assessed using immunohistochemistry (IHC) staining, according to the guidelines of the American Society of Clinical Oncology/College of American Pathologists [14, 15]. ER was scored as either positive or negative, with a 1% cut-off for nuclear immunostaining. HER2 positivity was defined as IHC 3+ or IHC 2+, and HER2 gene amplification using fluorescence in situ hybridization. Molecular subtypes of breast cancer were classified as luminal (ER-positive and HER2-negative), HER2-positive (ER-positive or ER-negative and HER2-positive), or triple-negative (ER-negative and HER2-negative). The luminal breast cancer types were classified as luminal A-like (Ki-67 labelling index <20%) and luminal B-like (Ki-67 labelling index ≥20%).

Statistical analysis

The data are presented as numbers (percentages) or medians (interquartile ranges, IQRs) unless otherwise indicated. Frequencies were compared using the chi-squared test for categorical variables. Continuous variables were compared using the Mann-Whitney *U* test or Kruskal-Wallis test. *P* values <0.05 were considered to be statistically significant. All statistical analyses were performed using EZR (Saitama Medical Center, Jichi Medical University, Saitama, Japan), which is a graphical user interface for R (The R Foundation for Statistical Computing, Vienna, Austria) [17].

Results

A total of 1,523 patients were assessed, and their clinicopathological characteristics are summarized in Table 1. In total, 81.6% had T1/T2 tumours and 13.1% had noninvasive carcinoma. Axillary lymph node metastases were present in 423 patients (27.8%), and LVI was present in 358 patients (23.5%). The molecular subtype distribution was as follows: luminal A-like in 463 patients (30.4%) luminal B-like in 661 (43.4%), HER2-positive in 229 (15.0%), and triple-negative in 157 (10.3%). The median

Table 4 Characteristics of patients with tumours of stages T2 to T4

Characteristic	Value
Age (years), median (range)	57 (23–90)
T status, *n* (%)	
T2	419 (27.5)
T3	45 (2.9)
T4	36 (2.4)
N status, *n* (%)	
N0	235 (47.0)
N1	183 (36.6)
N2	47 (9.4)
N3	35 (7.0)
Histology, *n* (%)	
Invasive carcinoma of no special type	439 (87.8)
Invasive lobular carcinoma	21 (4.2)
Other	40 (8.0)
Nuclear grade, *n* (%)	
1	43 (8.6)
2	167 (33.4)
3	290 (58.0)
Lymphovascular invasion, *n* (%)	
Negative	207 (41.4)
Positive	159 (31.8)
Unknown	134 (26.8)
Subtype, *n* (%)	
Luminal A-like	182 (36.4)
Luminal B-like	318 (63.6)
HER2-positive	316 (63.2)
Triple-negative	259 (51.8)

HER2 human epidermal growth factor receptor 2

SUVmax1, SUVmax2 and RI were 2.2 (1.4–4.1), 2.3 (1.3–4.6) and 2.6% (−9.2 to 15.0), respectively.

Table 2 and Fig. 1 show the relationships between the metabolic and biological parameters. Tumour size, nodal metastasis, histology, nuclear grade, LVI, and molecular subtype were significantly correlated with SUVmax1, SUVmax2 and RI (all $P < 0.001$). The SUVmax values were significantly lower in noninvasive carcinoma, microinvasive carcinoma, invasive lobular carcinoma and other histological types, than in invasive carcinoma of no special type ($P < 0.001$); this histological tumour type tended to exhibit negative RI values. The median SUVmax and RI gradually increased as the nuclear grade increased. The median SUVmax1, SUVmax2 and RI in the various molecular subtype were as follows: 1.6, 1.5 and 0% in luminal A-like, 2.5, 2.6 and 5.3% in luminal B-like, 3.1, 3.4 and 6.9% in HER2-positive, and 4.0%, 4.7% and 11.4% in triple-negative breast cancer. Negative RI was observed in Tis/T1 tumours, in the absence of nodal metastasis, in low-grade tumours, in tumours negative for LVI, and in luminal A-like tumours (Tables 2 and 3).

The cutoff value for background SUVmax1 was set at 1.4 based on the 75% percentile in the normal breast. In the low SUVmax1 group (<1.4), the relationship between the biological parameters and RI was poor, whereas in the high SUVmax1 group (≥1.4), RI was significantly correlated with large tumour size, lymph node metastasis, high tumour grade, positive LVI, and HER2-positive and triple-negative subtypes (all $P < 0.001$) (Table 3).

We also analysed the relationship between the metabolic and biological parameters in 500 patients with tumours of stages T2 to T4 to eliminate the influence of the partial volume effect (Tables 4 and 5). Metabolic parameters were correlated with nodal metastasis, histology, nuclear grade, and molecular subtype. Tumour status was correlated with SUVmax1 and SUVmax2. RI was useful in distinguishing invasive carcinoma of no special type, high nuclear grade, luminal B-like, HER2-positive, and triple-negative breast cancer.

Discussion

This study indicated that SUVmax1, SUVmax2 and RI determined using dual-phase FDG PET/CT were correlated with the biological parameters of breast cancer. A positive RI indicated malignant features when breast tumours had significant FDG accumulation. Many cancers, including breast cancer, show upregulation of glycolysis and FDG uptake [18]. High FDG uptake in primary breast tumour is associated with aggressive biological features. Previously, we have found that tumours with a high SUVmax are highly malignant and have a poor prognosis in patients with operable breast cancers [19]. Other studies have also shown that enhanced FDG uptake is correlated with malignant tumour biology and ER negativity [20–22]. FDG PET/CT may be a noninvasive tool for predicting the baseline risk of breast cancer before treatment.

Dual-phase FDG PET/CT is used to discriminate between benign and malignant diseases [9]. Although FDG uptake in benign or inflammatory lesions has been shown to reach a maximum within 30 min of FDG administration, malignant tumours have been shown to accumulate FDG for up to 4–5 h [6–8]. Some studies have assessed whether RI is related to biological characteristics in breast cancer [10–14]. Moon et al. found that high RI is associated with low ER expression and high HER2 expression [10]. García Vicente et al. found that RI is related to grade, HER2 status, Ki-67 labelling index, and ER, progesterone receptor and HER2 status [11, 12]. However, García Vicente et al. also found that RI cannot distinguish between molecular subtypes of breast cancer [13]. In

Table 5 Relationship between metabolic and biological parameters in patients with tumours of stage T2 to T4

Parameter	SUVmax1		SUVmax2		RI (%)	
	Median (IQR)	*P* value	Median (IQR)	*P* value	Median (IQR)	*P* value
T status		0.031		0.024		0.137
T2	4.2 (2.7–6.6)		4.7 (2.8–7.9)		12.2 (1.9–20.6)	
T3	4.6 (3.0–7.6)		5.3 (3.1–9.0)		13.9 (2.6–18.9)	
T4	5.6 (4.2–8.9)		6.7 (4.8–11.0)		15.6 (9.6–21.8)	
N status		0.005		0.003		0.012
N0	4.0 (2.4–6.5)		4.4 (2.5–7.5)		10.0 (0.0–19.5)	
N1	4.2 (2.9–6.8)		4.8 (3.2–8.1)		14.1 (6.0–20.5)	
N2	4.7 (3.2–7.1)		5.8 (3.5–8.5)		14.3 (0.0–21.1)	
N3	6.3 (4.3–8.8)		8.0 (4.6–10.6)		17.1 (7.4–26.9)	
Histology		<0.001		<0.001		<0.001
Invasive carcinoma of no special type	4.6 (2.9–7.2)		5.3 (3.0–8.8)		14.0 (4.6–21.1)	
Invasive lobular carcinoma	1.9 (1.3–3.0)		1.8 (1.2–3.0)		0.0 (−11.8 to 6.7)	
Others	3.2 (2.2–4.5)		3.3 (1.2–4.9)		6.0 (−8.5 to 12.8)	
Nuclear grade		<0.001		<0.001		<0.001
1	2.6 (1.7–5.7)		2.4 (1.4–6.4)		0.0 (−9.9 to 17.3)	
2	3.9 (2.6–5.8)		4.3 (2.8–6.8)		12.0 (0.0–19.3)	
3	5.0 (3.0–8.1)		5.6 (3.4–9.7)		14.0 (5.9–21.7)	
Lymphovascular invasion		0.856		0.972		0.101
Negative	4.0 (2.3–6.5)		4.7 (2.4–7.6)		11.1 (0.0–19.1)	
Positive	3.8 (2.6–6.0)		4.2 (2.8–7.1)		14.0 (3.7–20.0)	
Subtype		<0.001		<0.001		<0.001
Luminal A-like	2.8 (1.8–4.1)		2.8 (1.7–4.6)		4.8 (−7.7 to 16.0)	
Luminal B-like	4.0 (2.7–6.0)		4.5 (2.9–7.1)		12.3 (2.6–20.0)	
HER2-positive	5.6 (3.7–8.5)		6.4 (4.3–9.8)		15.8 (7.6–21.8)	
Triple-negative	7.2 (5.0–9.3)		8.3 (5.2–11.5)		16.3 (8.6–25.5)	

HER2 human epidermal growth factor receptor 2, *IQR* interquartile range, *RI* retention index, *SUVmax* maximum standardized uptake value

addition, Ozen et al. suggested that only progesterone receptor status is associated with RI [14]. Findings on the significance of RI in determining the biological features of breast cancer are inconsistent, and the numbers of patients in these studies were relatively small.

We included in this study a large cohort to clarify the significance of RI in breast cancer assessment. RI was correlated with the biological parameters as well as tumour SUVmax, which was significant in tumours with a high SUVmax. When the SUVmax of the primary tumour was equivalent to that of the normal breast, the change in SUVmax appeared to reflect variations in physiological accumulation in the mammary gland. Because our cohort included many patients with a small tumour (Tis 13.1%, T1 54.1%), the median SUVmax values were low and the partial volume effect might have affected the results [23]. Therefore, we further analysed patients with breast cancer of stages T2 to T4, in order to minimize the influence of the partial volume effect. Metabolic parameters were also correlated with nodal metastasis, histology, nuclear grade, and molecular subtype. Dual-phase FDG PET/CT identified tumours with a high nuclear grade and distinguished luminal A-like breast cancer from luminal B-like, HER2-positive and triple-negative breast cancers. Our findings confirm that dual-phase FDG PET/CT imaging is helpful for the adaptive selection of chemotherapy in early breast cancer.

This study had some limitations that were imposed by its retrospective design and the unknown clinical outcomes including treatment effect and prognosis. However, this large-cohort study provides important information on the diagnostic value of dual-phase FDG PET/CT.

Conclusion

RI determined using delayed-phase FDG PET/CT reflects the malignant features in breast cancers with significant FDG uptake. Dual-phase imaging was helpful in distinguishing luminal A-like breast cancer from luminal B-like, HER2-positive and triple-negative breast cancers.

Acknowledgments The authors thank Kazushi Marukawa and Masatsugu Tsujimura of Chuden Hospital for providing data regarding PET examinations. The authors also thank Ai Shimamoto for data management.

Compliance with ethical standards

Conflicts of interest None.

Ethical approval All procedures performed in studies involving human participants were in accordance with the ethical standards of the institutional research committee and with the principles of the 1964 Declaration of Helsinki and its later amendments or comparable ethical standards.

Informed consent For this type of study, formal consent is not required.

Publisher's Note Springer Nature remains neutral with regard to jurisdictional claims in published maps and institutional affiliations.

References

1. Siegel RL, Miller KD, Jemal A. Cancer statistics, 2017. CA Cancer J Clin. 2017;67:7–30.
2. Curigliano G, Burstein HJ, PW E, Gnant M, Dubsky P, Loibl S, et al. De-escalating and escalating treatments for early-stage breast cancer: the St. Gallen International Expert Consensus Conference on the Primary Therapy of Early Breast Cancer 2017. Ann Oncol. 2017;28:1700–12.
3. Goldhirsch A, Wood WC, Gelber RD, Coates AS, Thurlimann B, Senn HJ. Progress and promise: highlights of the international expert consensus on the primary therapy of early breast cancer 2007. Ann Oncol. 2007;18:1133–44.
4. Hong S, Li J, Wang S. 18FDG PET-CT for diagnosis of distant metastases in breast cancer patients. A meta-analysis. Surg Oncol. 2013;22:139–43.
5. Groheux D, Espie M, Giacchetti S, Hindie E. Performance of FDG PET/CT in the clinical management of breast cancer. Radiology. 2013;266:388–405.
6. Boerner AR, Weckesser M, Herzog H, Schmitz T, Audretsch W, Nitz U, et al. Optimal scan time for fluorine-18 fluorodeoxyglucose positron emission tomography in breast cancer. Eur J Nucl Med. 1999;26:226–30.
7. Lodge MA, Lucas JD, Marsden PK, Cronin BF, O'Doherty MJ, Smith MA. A PET study of 18FDG uptake in soft tissue masses. Eur J Nucl Med. 1999;26:22–30.
8. Hamberg LM, Hunter GJ, Alpert NM, Choi NC, Babich JW, Fischman AJ. The dose uptake ratio as an index of glucose metabolism: useful parameter or oversimplification? J Nucl Med. 1994;35:1308–12.
9. Kumar R, Loving VA, Chauhan A, Zhuang H, Mitchell S, Alavi A. Potential of dual-time-point imaging to improve breast cancer diagnosis with (18)F-FDG PET. J Nucl Med. 2005;46:1819–24.
10. Moon H, Noh WC, Kim HA, Kim EK, Park KW, Lee SS, et al. The relationship between estrogen receptor, progesterone receptor and human epidermal growth factor receptor 2 expression of breast cancer and the retention index in dual phase (18)F-FDG PET/CT. Nucl Med Mol Imaging. 2016;50:246–54.
11. García Vicente AM, Castrejón ÁS, Relea Calatayud F, Muñoz AP, León Martín AA, López-Muñiz IC, et al. 18F-FDG retention index and biologic prognostic parameters in breast cancer. Clin Nucl Med. 2012;37:460–6.
12. García Vicente AM, Soriano Castrejón A, Relea Calatayud F, Muñoz Madero V, Molina Garrido MJ, León Martín AA, et al. 18F-FDG semi-quantitative parameters and biological prognostic factors in locally advanced breast cancer. Rev Esp Med Nucl Imagen Mol. 2012;31:308–14.
13. García Vicente AM, Soriano Castrejón Á, León Martín A, Chacón López-Muñiz I, Muñoz Madero V, Muñoz Sánchez Mdel M, et al. Molecular subtypes of breast cancer: metabolic correlation with (1)(8)F-FDG PET/CT. Eur J Nucl Med Mol Imaging. 2013;40:1304–11.
14. Ozen A, Altinay S, Ekmekcioglu O, Albayrak R, Muhammedoglu A, Yigitbas H, et al. Dual-time (18)F-FDG PET/CT imaging in initial Locoregional staging of breast carcinoma: comparison with conventional imaging and pathological prognostic factors. Indian J Surg. 2016;78:382–9.
15. Edge SB, Byrd DR, Compton CC, Fritz AG, Greene F, Trotti A. AJCC cancer staging manual. 7th ed. New York: Springer; 2010.
16. Japanese Society of Nuclear Medicine. FDG-PET, PET/CT clinical practice guideline. 2012 (in Japanese). http://jsnm.sakura.ne.jp/wp_jsnm/wp-content/themes/theme_jsnm/doc/fdgpet_guideline2012_120912.pdf. Accessed 7 Jan 2019.
17. Kanda Y. Investigation of the freely available easy-to-use software 'EZR' for medical statistics. Bone Marrow Transplant. 2013;48:452–8.
18. Gatenby RA, Gillies RJ. Why do cancers have high aerobic glycolysis? Nat Rev Cancer. 2004;4:891–9.
19. Kadoya T, Aogi K, Kiyoto S, Masumoto N, Sugawara Y, Okada M. Role of maximum standardized uptake value in fluorodeoxyglucose positron emission tomography/computed tomography predicts malignancy grade and prognosis of operable breast cancer: a multi-institute study. Breast Cancer Res Treat. 2013;141:269–75.
20. Ekmekcioglu O, Aliyev A, Yilmaz S, Arslan E, Kaya R, Kocael P, et al. Correlation of 18F-fluorodeoxyglucose uptake with histopathological prognostic factors in breast carcinoma. Nucl Med Commun. 2013;34:1055–67.
21. Groheux D, Giacchetti S, Moretti JL, Porcher R, Espie M, Lehmann-Che J, et al. Correlation of high 18F-FDG uptake to clinical, pathological and biological prognostic factors in breast cancer. Eur J Nucl Med Mol Imaging. 2011;38:426–35.
22. Ueda S, Tamaki Y, Yano K, Okishiro N, Yanagisawa T, Imasato M, et al. Cosmetic outcome and patient satisfaction after skin-sparing mastectomy for breast cancer with immediate reconstruction of the breast. Surgery. 2008;143:414–25.
23. Soret M, Bacharach SL, Buvat I. Partial-volume effect in PET tumor imaging. J Nucl Med. 2007;48:932–45.